Available online at www.CivileJournal.org

Civil Engineering Journal

(E-ISSN: 2476-3055; ISSN: 2676-6957)

Vol. 9, No. 12, December, 2023

Optimization Studies of Iron Ore Tailings Powder and Natural Zeolite as Concrete Admixtures

Mahmoud Al-Khazaleh [1], P. Krishna Kumar [2*]

[1] *Munib and Angela Masri Faculty Engineering, Aqaba University of Technology, Jordan.*

[2] *Department of Civil Engineering, Francis Xavier Engineering College, Tirunelveli 627003, India.*

Received 20 August 2023; Revised 06 October 2023; Accepted 02 November 2023; Published 01 December 2023

Abstract

The disposal of Iron ore tailings Powder (IP) is the primary concern for numerous steel industries. Similarly, natural zeolite, a significant by-product of volcanic eruptions, pollutes the environment to an extreme degree. This study investigates and implements the extensive use of IP and natural zeolite as admixtures in M20-grade concrete in order to address the challenges posed by IP and zeolite. By varying the admixture percentage, three distinct mix ratios were formed. First, sand was replaced by iron at concentrations of 5%, 10%, 15%, and 20%. Second, cement was replaced by zeolite at 5%, 10%, 15%, and 20%. In the final mixture, both sand and cement were substituted with iron ore powder and zeolite, respectively, at 5%, 10%, 15%, and 20%. Conplast SP 430, a water-reducing admixture, was used in all of the mixtures at 1% by weight of cement. The mechanical properties of concrete, including compressive strength, split tensile strength, and flexural strength, were studied. To evaluate the long-term properties of admixture-modified concrete, durability tests such as permeability tests, water absorption tests, rapid chloride attack tests, acid attack tests, and sulphate attack tests were conducted. In addition, slump cone tests and thermal conductivity tests were conducted on all the mix combinations to determine the changes in workability and thermal conductivity coefficient. The test results demonstrated that a mix containing 10% zeolite replaced with cement and 10% iron ore tailing powder replaced with sand has the highest performance in terms of strength and durability characteristics. The study also constructs a comparable cost estimate to ensure that its actual implementation is feasible.

Keywords: Iron Ore Tailing Powder; Natural Zeolite; Thermal Conductivity; Workability; RCPT; Cost Analysis.

1. Introduction

The substantial market demand for iron-based components necessitates the extraction of iron ore from mines, even when the ore contains a lower iron content. A significant quantity of non-utilizable ore, classified as trash, has been duly recorded [1]. In the year 2019, nations known for their significant iron production, namely Australia, India, and China, collectively generated 1.5 billion tons of iron. However, it is worth noting that during this period, a substantial amount of waste iron ore powder, totaling 2.5 billion tons, was deposited. India accounts for around 10–25% of the gross quantity of iron ore extraction worldwide [2, 3]. The disposal of iron ore tailings is a significant environmental concern. The pre-treatment process of iron ore tailings incurs significant expenses. The global yearly expenditure for the accumulation of iron ore tailings was anticipated to exceed 2.2 billion US dollars [4]. The treatment and efficient use of iron ore tailings have posed significant environmental challenges, hence presenting a crucial obstacle for the iron ore-mining sector in achieving sustainability [5]. The global utilization potential of IP is significantly limited, and it is creating a serious

* Corresponding author: krishnakumarpalaniappan1991@gmail.com

http://dx.doi.org/10.28991/CEJ-2023-09-12-08

problem by contaminating the quality of soil, air, and water [6]. However, few studies indicate that the advantageous physical and chemical properties of IP were widely utilized in the manufacturing of ceramics [3, 7, 8], bricks [9, 10], and backfill materials [11]. Several researchers have undertaken studies to investigate the suitability of using IP as a substitute for fines in concrete, owing to its rough texture and smaller particle size in comparison to other pozzolanic mineral admixtures [12–14]. However, the existing studies have not effectively demonstrated the long-term durability changes in concrete. As evidence of the ongoing study on using tailing waste as a mineral additive in concrete, several researchers have also examined the viability of various types of tailings, including tungsten, phosphates, and copper tailings [12].

Zeolites, a class of minerals characterized by their hydrated alumino-silicate composition, are derived from volcanic rocks [15]. Clinoptilolite, heulandite, analcime, chabazite, and mordenite are highly prevalent zeolite minerals found in nature. The clinoptilolite zeolite contains high lime reactivity, similar to that of silica fume and greater compared to that of fly ash and a non-zeolitic natural pozzolan, as reported [16]. Huge concentrations of active SiO_2 and AI_2O_3 in zeolite react with the $Ca(OH)_2$ produced by the hydration process of cement to form additional CSH gel, thereby enhancing the strength of hardened concrete [17]. Numerous studies have documented the advantageous use of zeolite as a substitute for cement in various applications. This substitution has been found to significantly improve the mechanical robustness and durability properties of concrete, mostly due to the notable pozzolanic activity of zeolite [18–20]. The presence of microspores and mesopores in zeolites contributes to their possession of a significant specific surface area. Consequently, the increased water requirement leads to a decrease in the slump of concrete. Furthermore, water absorption is enhanced because of the existence of montmorillonite clay residues. The process of calcination induces dehydroxylation in zeolite, resulting in the alteration of the clay particles and subsequent deformation of the zeolite structure. This deformation ultimately leads to a reduction in the water absorption capacity of zeolite [21]. Excessive calcination of zeolites also leads to a decrease in reactivity. Nevertheless, when zeolites were subjected to calcination temperatures of 800°C, no detrimental impacts on their reactivity were seen [22]. The use of zeolite as a replacement for cement in concrete not only enhances its structural integrity but also has the potential to mitigate carbon dioxide emissions, therefore yielding environmental advantages.

There is a noticeable increase in the quantity of research studies that are specifically dedicated to investigating the utilization of IP and natural zeolite in the context of concrete infrastructure. Few studies document that mechanical activation is performed to obtain well-graded IP and increase specific surface area. The mechanical activation of IP is accomplished through a continuous gridding process occurring at varying time intervals [12]. During the pre-treatment phase, the aforementioned procedure requires a substantial amount of energy and incurs significant costs. Therefore, eliminating the mechanical activation of IP and disposing of iron ore residue powder in concrete will preserve the environment and aid in its preservation. It was attempted to incorporate IP and fine zeolite into the concrete. No previous research has attempted to combine the analysis of using calcined natural zeolite as a cement substitute and non-mechanically activated IP as a fine aggregate. The purpose of this investigation is to examine the mechanical properties and long-term performance characteristics of mineral-admixed concrete.

In this study, the effects of replacing cement with calcined natural zeolite and fine aggregate with iron ore tailing powder on the mechanical strength and durability properties of concrete were examined. A cost-benefit analysis was conducted on the optimal combination with the highest performance, which describes the adaptability of using non-usable iron ore tailings and zeolite to reduce the cost of concrete and the environmental hazards associated with cement use.

2. Material and Methods

Ramco Cement Limited, Tirunelveli, supplied the OPC 53-grade cement for this investigation. Crushed sand with a maximum size of 4.75 mm, a specific gravity of 2.65, a unit weight of 1750 kg/m^3, and coarse aggregate with a maximum size of 19 mm were utilized. The grading of aggregates and admixtures was as per the requirements of IS 383:1970, as shown in Figure 1. The water-to-cement ratio of 0.5 was adopted for all the mixes. Conplast SP 430 was used as a water-reducing admixture in the mix. The natural zeolites were calcined in 50-gram samples. The temperature was raised from ambient to 800°C over the course of 160 minutes at a rate of approximately 5°C per minute. Once the temperature reached 800°C, it remained stable for 5 hours. The temperature was then gradually reduced to room temperature over the course of 160 minutes at a rate of approximately 5°C per minute. Figure 2 depicts the XRD images of natural zeolite before and after calcination. The intensity count of clinoptilolite in calcinated zeolite was less than that of ordinary zeolite. This was due to the collapse of the structural lattice of the zeolite mineral due to heating [15]. The iron ore tailing powder was collected from the iron ore mining industry in Kanjamalai, Salem. The chemical composition of cement, calcined zeolite, iron ore tailings powder, and sand is shown in Table 1. Table 2 shows the physical properties of the raw materials used.

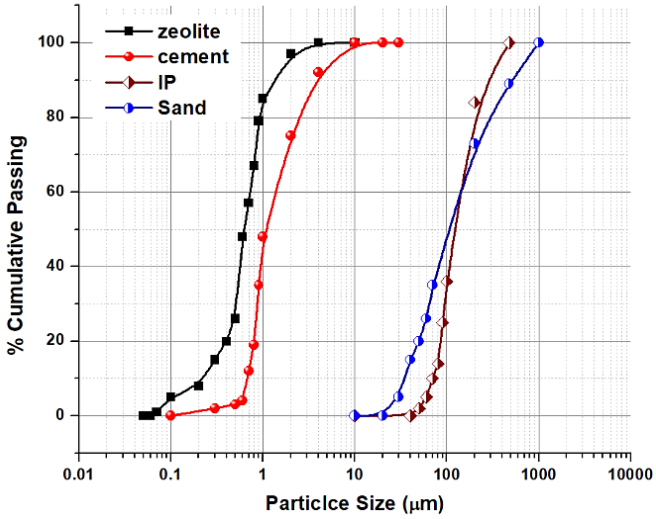

Figure 1. PSD curve of raw materials used

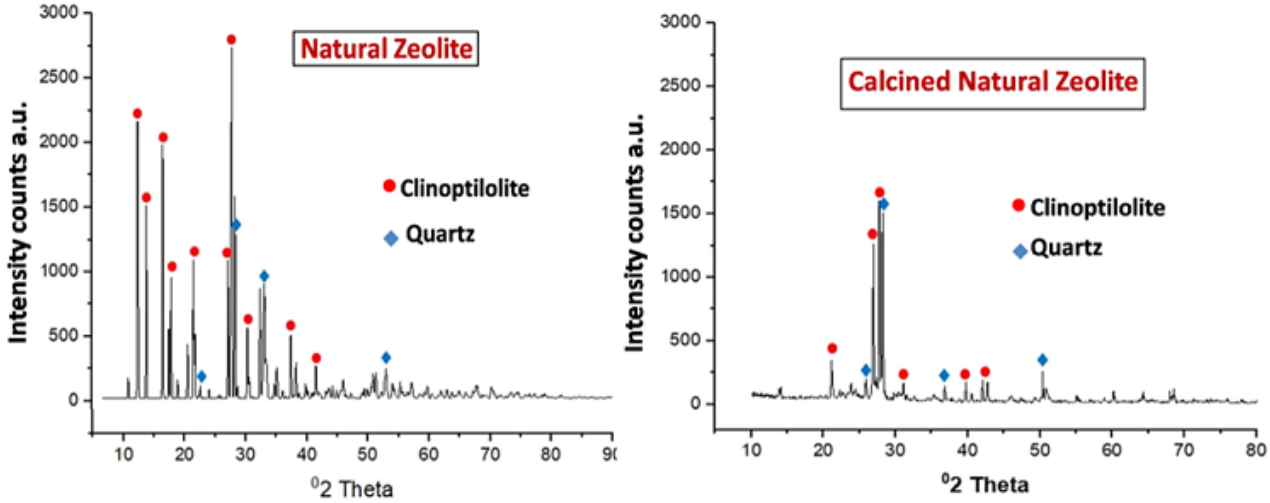

Figure 2. XRD images of zeolite before and after calcination

Table 1. Chemical composition of raw materials

	SiO_2	Al_2O_3	CaO	Fe_2O_3	MgO	SO_3	K_2O	Na_2O	LOI
Cement	20.8	5.1	63.27	3.87	2.26	2.12			2.52
Zeolite	63.38	10.43	3.56	0.49	0.5	0.005	1.27	6.8	13.565
Iron Powder		-	-	99	-	-	-	-	1
Sand	93	1	0.4	0.5	0.8	0.5	-	-	3.8

Table 2. Physical properties of raw materials

	D_{10}	D_{50}	D_{90}	water absorption	Specific Gravity	Fineness Modulus
Cement	2.56	4.32	6.92	-	3.12	3.1
Zeolite	0.2	0.68	1.08	-	2.48	2.85
Iron Powder	30	100	200	-	3.5	3.15
Fine Aggregate	30	70	475	1.98	2.58	3.4
Coarse Aggregate	-	-	19	0.66	2.69	-

Figure 3 shows the flowchart of the research methodology through which the objectives of this study were achieved.

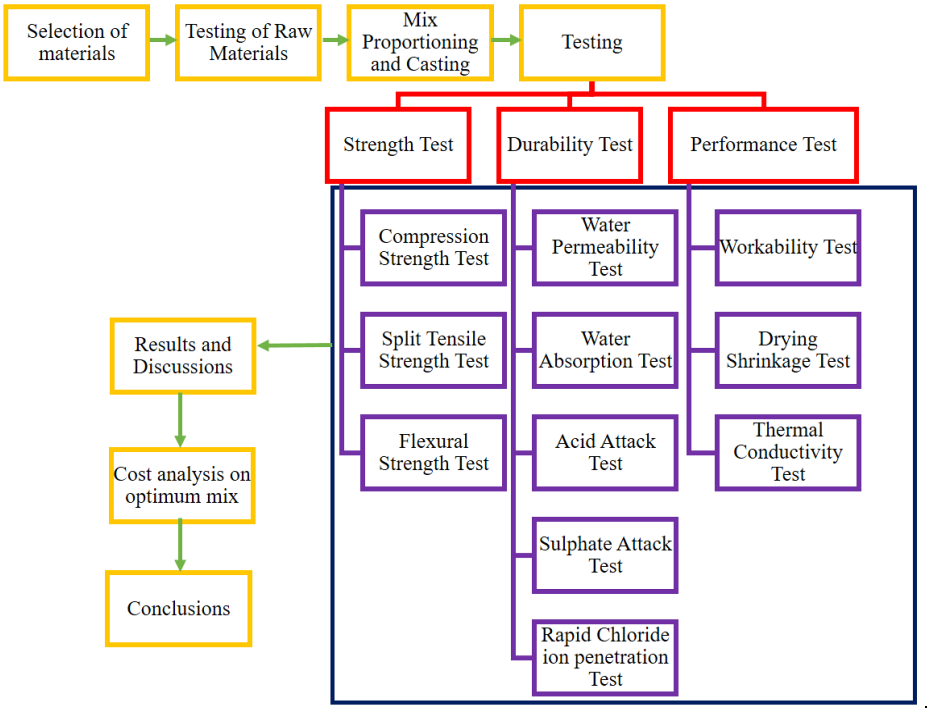

Figure 3. Research methodology flowchart

2.1. Mix Proportioning and Casting

The conventional concrete mix proportions were determined in accordance with IS 10262:2009. Table 3 displays the proportional breakdown of the mix ratios adopted. The label for concrete formulations was divided into four distinct sections. Conventional concrete, denoted as reference (REF), was the first series. The admixture-modified concrete test results were compared with the control mixture. The second section contains IP as fine aggregate replacement in proportions of 5%, 10%, 15%, and 20%, represented as IP (correspondent replacement percentage). The third section contains zeolite as a replacement for cement at percentages of 5%, 10%, 15%, and 20%, denoted by Z (correspondent replacement percentage). In the last category, iron ore tailing powder and zeolite were combined at 5%, 10%, 15%, and 20% as replacements for both fine aggregate and cement, respectively, represented as IPZ (correspondent replacement percentage). A laboratory drum mixer was used to produce the concrete mix. Initially, coarse aggregate and fine aggregate were added, followed by the cement, which was allowed to mix for two to three minutes in the dry state. In the case of concrete containing iron powder, the iron powder was allowed to mix during the initial dry mixing with the fine aggregate. In the case of zeolite substitution, the calculated amount of zeolite is added to the total amount of superplasticizer and thoroughly mixed before being dissolved in the calculated volume of water. Further zeolite is added to the mixer and mixed for an additional three minutes. This method was used to achieve a homogeneous mixture and uniform dispersion of zeolite in the concrete [23]. The mechanical and durability properties of admixture-modified concrete were determined by casting and testing nine cubes of 150×150×150 mm, three prisms of 150×150×1000 mm, and three cylinders of 150×300 mm for each mix ID. Hence, in total, 117 cubes, 39 cylinders, and 39 cubes were cast.

Table 3. Design mix proportions of concrete mixtures

Series	Mix ID	Cement (kg/m^3)	Sand (kg/m^3)	Coarse Aggregate (kg/m^3)	Water (kg/m^3)	Zeolite (kg/m^3)	Iron Powder (kg/m^3)	SP (kg/m^3)
Conventional concrete	Ref	420	624	1218	168	-	0	4.2
Iron Powder	IP5	420	592.5	1218	168	-	31.5	4.2
	IP10	420	561	1218	168	-	63	4.2
	IP15	420	529.5	1218	168	-	94.5	4.2
	IP20	420	498	1218	168	-	126	4.2
Zeolite	Z5	399	630	1218	168	21	-	4.2
	Z10	378	630	1218	168	42	-	4.2
	Z15	357	630	1218	168	63	-	4.2
	Z20	336	630	1218	168	84	-	4.2
Zeolite and Iron Powder	IPZ5	399	592.5	1218	168	21	31.5	4.2
	IPZ10	378	561	1218	168	42	63	4.2
	IPZ15	357	529.5	1218	168	63	94.5	4.2
	IPZ20	336	498	1218	168	84	126	4.2

2.2. Experimental Program

The workability of conventional and admixture-modified concrete was estimated by conducting slump tests. The plastic density and dry density of the specimens were determined as per IS 1199:1959. The compressive strength was evaluated on 150-mm cube samples after a 28 and 90-day curing period. The tensile strength of the concrete was estimated by performing a split tensile strength test on cylinders of 300mm length and 150mm diameter after 28 days of curing. The 28-day flexural strength test was conducted on a concrete prism (1000×150×150 mm) following IS 516:1959. The water absorption test was performed as per ASTM C642-13, following Equation 1.

$$\%\ \text{of water absorption} = \frac{(\text{Ws}-\text{Wd})}{\text{Wd}} \times 100 \quad (1)$$

where W_s is Saturated weight of cube after 24 hours immersion in water, and W_d is dry weight of cube.

The constant head permeability test was conducted on 150-mm cubes to determine the coefficient of permeability in accordance with IS 3085: 1965. The coefficient of permeability was calculated as shown in Figure 4 following Equation 2. The 28-day-cured 150-mm cube samples were oven-dried, and water pressure was applied normal to the surface of the cube in a permeability apparatus. After three days, the change in porosity of the specimen was examined

$$K = \frac{q}{at\frac{h}{T}} \quad (2)$$

where K is Permeability Coefficient, q is Quantity of water percolating throughout the test period (cm^3/sec), a is Cross sectional area of specimen (cm^2), t is Time (sec), h is Pressure head (m), and T is Specimen thickness (m).

To evaluate the amount of deterioration in the concrete, 150-mm cube specimens were tested for accelerated sulphate attack and acid attack test. 150-mm concrete cubes are submerged in a solution containing 5% $MgSO_4$ and 5% Na_2SO_4 by weight of water for the sulphate attack test. For the acid attack test, a solution containing H_2SO_4 with a pH of 2 was used. The 150-mm cubes were immersed in the corresponding solution for 28 days, 90 days, and 120 days to determine the loss in compressive strength and percentage of weight loss in accordance with ASTM C 267-01. The percentage loss in compressive strength was calculated as per Equation 3.

$$\text{Compressive strength loss}\ (\%) = \frac{[\text{Fc}-\text{Fcs}]}{\text{Fc}} \times 100 \quad (3)$$

where F_c is compressive strength of cubes (MPa), and F_{cs} is compressive strength of cubes subjected to sulphate /acid environment (MPa).

The 28-day-cured 150-mm cubes were subjected to a non-destructive ultrasonic pulse velocity test per ASTM C597-07 (ASTM 2016) guidelines. The thermal conductivity of a concrete was determined by conducting a heat flow test as shown in Figure 4 on a 150-mm cube specimen using Equation 4 in accordance with the standards of IS 9489:1980 (BSI 1980).

$$k = \frac{W}{a}[1 \times \frac{T}{\Delta t}] \quad (4)$$

where a is surface area of cube in contact with hot or cold plates (mm^2), T is Thickness of the specimen (mm), W is electric power in Watt, Δt is difference in temperature between hot and cold plates.

The chloride ion penetration test was conducted as per ASTMC 1202. The chloride ion penetration was evaluated as a total charge passed measured in coulombs over a 6-hour measurement period. A cylindrical specimen was divided to a thickness of 50 mm and subjected to a saturated vacuum for 7, 28, and 90 days. The specimens were confined in two-cell chambers; one cell contained 0.3 M NaOH and the other contained a 3% NaCl solution. A 60-volt DC voltage was administered for six hours. Using a data recorder, the current that passed was measured every 30 minutes for six hours. According to the ASTM C1202 standard, the total charge transmitted was estimated and found to be proportional to the specimen's resistance to chloride ion penetration.

Figure 4. Thermal conductivity test setup

According to ASTM C157, the drying shrinkage test was conducted on 40×40×160 mm concrete prisms. In this investigation, two-gauge studs were positioned 160 mm apart on the specimen. Using a length comparator as shown in Figure 5, the length variation of the specimen was noted. The measurement was recorded to the nearest 0.002 mm at 7, 28, and 90 days.

Figure 5. Length comparator test setup

3. Results and Discussion

3.1. Workability Test

Figure 6 demonstrates the efficacy of concrete mixtures using varying quantities of replacement additives, as shown by their corresponding slump values. The findings indicate that the incorporation of admixtures in substitution of cement and sand leads to a decrease in slump values, implying a decrease in the workability of the concrete as compared to the control mixture. The usage of IP and Z resulted in the most unfavorable degree of operability. The IPZ-20 combination exhibited a significant decrease in slump, resulting in a reduction of 52.5% compared to the control mixture. The underlying cause of these phenomena can be traced to the enhanced water-absorption capacity demonstrated by zeolite and IP. The high specific surface area demonstrated by zeolite particles was the cause of the increase in the amount of water demand in the mixture [17]. Numerous investigations have demonstrated that the substitution of sand with iron ore tailing powder in concrete results in an elevated water demand within the mixture [6, 24]. In contrast, the combination using IP as a replacement for sand exhibited a more pronounced reduction in slump compared to the mixture incorporating Z replacements. The increased replacement quantities of the IP, which were substituted with sand, account for this phenomenon. The incorporation of IP as a replacement for 20% of the sand in traditional concrete leads to a significant decrease of 41.5% in slump, while the substitution of 20% of the cement with zeolite in conventional concrete results in a slump reduction of 33%. The graph depicts a clear correlation between the dose of admixture and the decrease in concrete slump values, showing a linear relationship. Nevertheless, the decrease in slump falls within the category of mild slump, as outlined in the IS 456:2000 standard. This highlights its suitability for applications involving heavily reinforced beam columns and slabs.

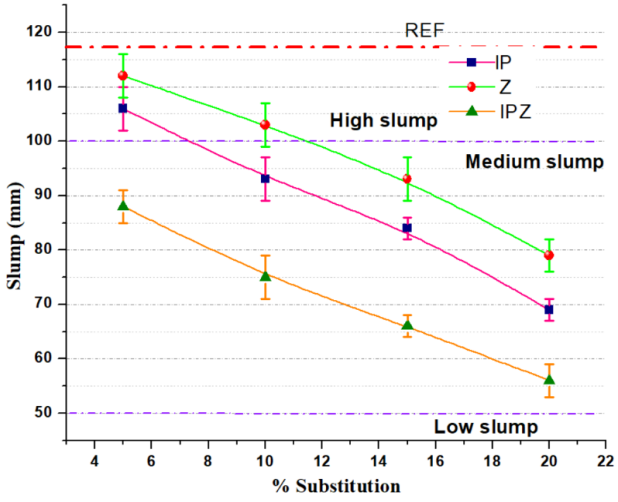

Figure 6. Slump value vs admixture substitution

3.2. Compression Strength Test

Figure 7 displays the compressive strength test results for concrete samples using IP, zeolite, IPZ, and conventional concrete. The test findings demonstrate that the substitution of sand with IP leads to a notable enhancement in the strength of the concrete across all curing periods. At 28 days of curing, the compressive strength of IP concrete exhibited a percentage increase relative to the control concrete. The replacement levels of 5%, 10%, 15%, and 20% resulted in percentage increases of 2.19%, 2.38%, 8.73%, and 10.88%, respectively. Similar to the 30-day curing period, the compressive strength for the 90-day curing period was 6.30, 6.65, 12.92, and 13.46% more than the standard mix. The observed enhancement in strength can be largely ascribed to the reduced particle size of IP, which effectively fills the gaps in concrete and optimizes the pore structure. Limited research suggests that an increase in iron concentration is associated with an increase in achieved strength [25]. The presence of a rough and angular structure in IP enhances the interaction bond between cement and aggregate interfaces, resulting in an enhancement of mechanical strength [26]. The increased strength observed at a later age can be attributed to the secondary reaction of free $Ca(OH)_2$ that occurs during cement hydration and the IP, leading to the formation of additional CSH gel. This phenomenon contributes to the enhancement of later-age strength [3]. Goyal et al. (2015) demonstrated that the inclusion of IP in concrete resulted in a similar growing trend in compressive strength. However, their investigation also revealed that a significant amount of IP in the concrete led to a loss in strength, mostly attributed to a lack of mix integrity [27].

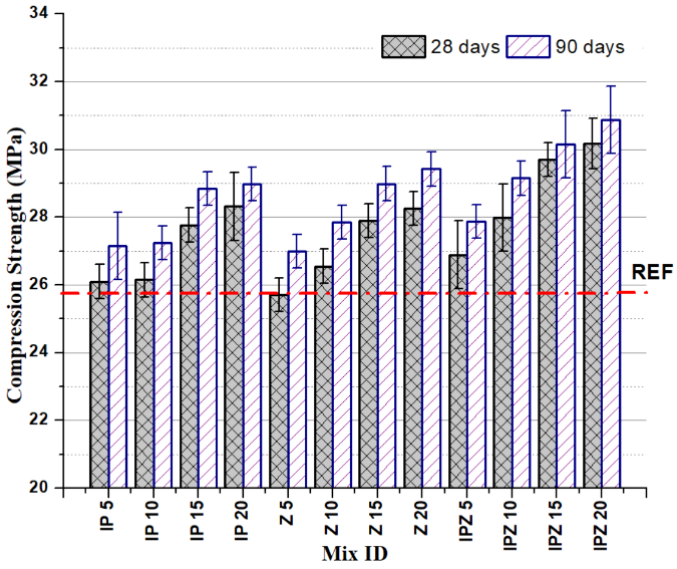

Figure 7. Compressive strength of various concrete mix

The incorporation of zeolite in concrete as a substitute for cement at varying proportions of 5%, 10%, 15%, and 20% has demonstrated an enhancement in the compressive strength of the concrete after 28 days. Specifically, the strength of the concrete rose by 0.82%, 3.95%, 9.2%, and 10.24%, respectively, corresponding to the aforementioned zeolite substitution percentages. Vaičiukynienė et al. (2012) experimentally proved the enhancement in strength of concrete up to 15% with increased natural zeolite concentration. This was attributed to the pozzolanic activity exhibited by natural zeolite, leading to the formation of supplementary hydro-aluminate gels inside the concrete [28]. The percentage increases in compressive strength with 5%, 10%, 15%, and 20% zeolite during the 90-day curing period were 5.71%, 9.04%, 13.50%, and 18.05%, respectively. The observation was made that the substitution of cement with zeolite leads to a noticeable enhancement in compressive strength. The clinoptilolite zeolite exhibits elevated concentrations of reactive SiO_2 and Al_2O_3, which undergo chemical reactions upon encountering calcium hydroxide generated during cement hydration. The aforementioned chemical process leads to the generation of supplementary calcium silicate hydrate (CSH) gel and aluminates, both of which play a significant role in enhancing the mechanical strength of the concrete. Therefore, the calcinated natural zeolite was deemed to possess characteristics indicative of a superior additional cementitious material. The incorporation of zeolite as a replacement for cement, together with the substitution of fine aggregate with IP, resulted in significantly higher compressive strength when compared to the other two series of mixtures. The compressive strength showed a respective increase of 9.16%, 14.13%, 18.05%, and 20.9% for IPZ. The percentages of the observed values were 5%, 10%, 15%, and 20% after a 28-day curing period.

The observed decrease in the rate of growth at higher replacement levels can be attributed to the reduced cement concentration in the mixture. The availability of free $Ca(OH)_2$ for secondary hydration decreases proportionally with the reduction in cement content. The surplus zeolite and IP remained unreacted and did not contribute to the hydration process. Nevertheless, these compounds function as additives inside the mixture, enhancing both its density and strength. The test conducted on UPV also demonstrated the enhancement of concrete integrity when including IPZ. Figure 8

displays the test findings pertaining to dry density and ultrasonic pulse velocity (UPV). The substitution of admixtures in concrete leads to an increase in both the wave propagation velocity and dry density. The IPZ 20 had the highest density and ultrasonic pulse velocity (UPV) values. This observation suggests that a state of uniformity was attained in the concrete mixture, characterized by optimal particle packing.

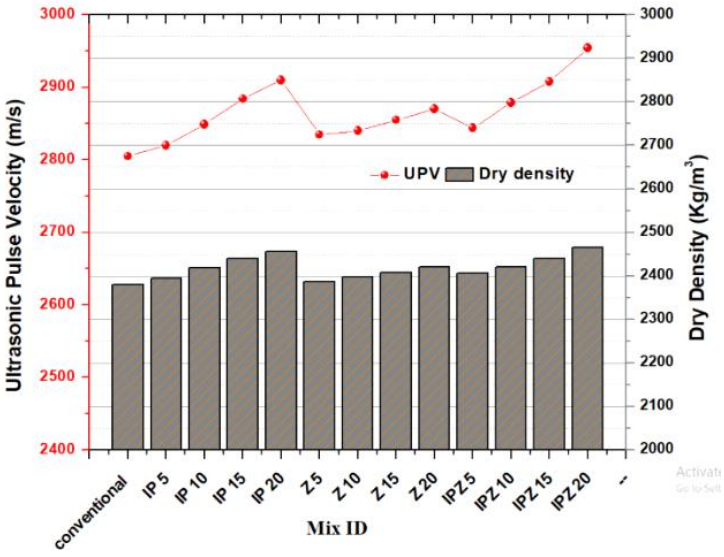

Figure 8. Dry density and UPV values of various concrete mix

3.3. Split Tensile Strength & Flexural Strength Test

Figure 9 displays the split tensile strength and flexural strength of the various concrete mixtures. In each mix series, it was observed that the split tensile and flexural strengths exhibited an increase in correlation with the rise in additive concentration as compared to traditional concrete. Nevertheless, the use of zeolite as a substitute for cement, at a maximum proportion of 15%, exhibited a moderate augmentation, which subsequently diminished with higher levels of substitution. The decrease in strength exhibited some ambiguity and may perhaps be ascribed to the agglomeration of zeolite particles or a deficiency in pozzolanic reactivity. However, it is worth noting that the compressive strength was somewhat elevated at this particular level of replacement. This observation indicates a deficiency in the bonding properties of concrete that incorporates zeolite. The IPZ concrete mix, when used in conjunction with IP concrete, exhibited a gradual improvement in both split tensile strength and flexural strength. The observed outcome can be attributed to an improvement in particle arrangement between the IP and zeolite. The test findings indicate that the combination of zeolite and IP exhibits the highest efficacy as a replacement for conventional concrete, as evidenced by increased concrete density and enhanced pozzolanic behavior. The observed trend in test findings exhibited a significant degree of comparability and relevance when compared to previous investigations conducted on concrete using both IP and macro-synthetic fibers [29].

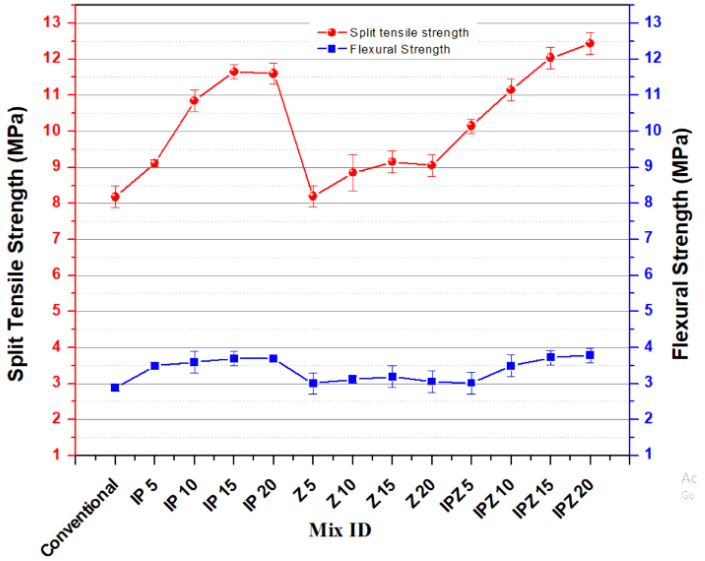

Figure 9. Split tensile strength and flexural strength of concrete mix

3.4. Permeability Test

The permeability of concrete was seen to decrease with an increase in additive replacement, as depicted in Figure 10. The permeability coefficient of IP20 concrete shows a reduction of 46.84% when compared to conventional concrete. Similarly, Z20 concrete demonstrated a reduction of 49.6%, while IPZ20 concrete exhibited the highest reduction at 55.2% when compared to conventional concrete. The IPZ20 combination had the lowest permeability coefficient when compared. The observed trend suggests that as the concentration of IPZ increased, there was a corresponding decrease in void content. This finding is consistent with a rise in the density of the mixture and improved particle packing. Zang et al. (2023) demonstrated that including IP as a substitute for up to 30% of the fine aggregate in concrete enhances its compressive strength. Moreover, this substitution leads to a significant reduction in concrete porosity, resulting in impermeable behavior [30].

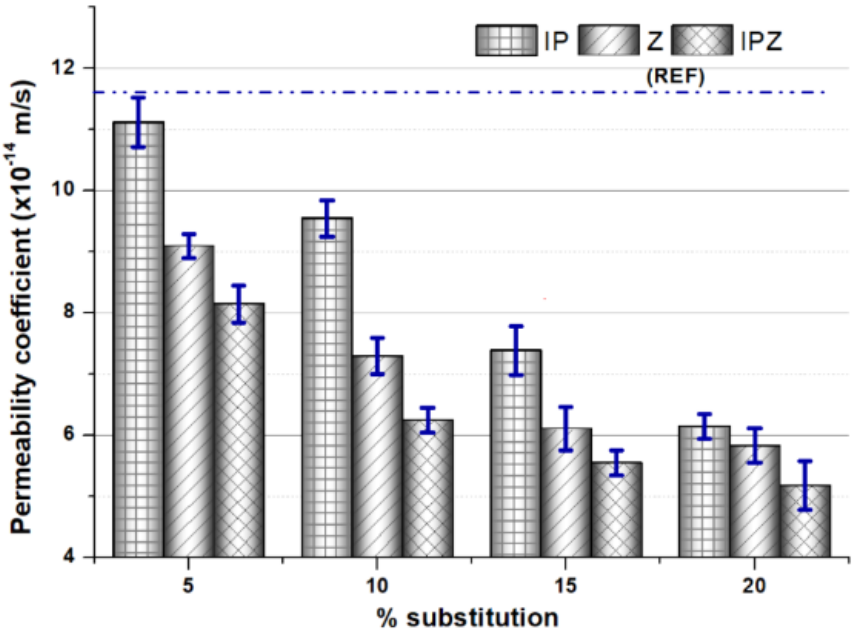

Figure 10. Permeability coefficient vs. admixture concentration

3.5. Water Absorption Test

Figure 11 illustrates the outcomes of water absorption experiments carried out following 7, 28, and 90 days of the curing process. The test findings suggest that the water absorption of IP concrete was lower compared to the concrete using zeolite. In all mix configurations, the rate of water absorption exhibited an increase after a curing period of 7 days, followed by a considerable drop after a curing period of 90 days. The water absorption rate of IPZ 20 samples, after being cured for 7 days, exhibited a 15.45% increase in comparison to conventional concrete samples. On the other hand, it was observed that the water absorption of samples cured over a period of 90 days exhibited an increase of 7.63% compared to conventional concrete. This shows that as the cure time increased, the rate of water absorption decreased. The absorption capacity of IPZ and zeolites was reduced due to the presence of water in the micro and macro pores on their surfaces during the curing process. The secondary phase of hydration may potentially lead to a decrease in water absorption. Similar findings in concrete with ceramic waste as coarse aggregate were achieved, and the study discovered that higher water absorption had a negative impact on the material's strength, workability, and durability attributes [31].

Interestingly, the water absorption of concrete containing zeolite was found to be the highest due to the larger macro voids formed during the mixing process, in comparison to other types of concrete. This leads to a higher level of water absorption. The decrease in permeability and the augmentation in water absorption rate of concrete incorporating zeolite and IP can be attributed to the elevated surface area of the zeolite and IP, which has the capacity to retain substantial quantities of surface water. Meanwhile, the reduced permeability can be attributed to a diminished number of interconnected pores within the concrete. Valipour et al. (2013) conducted a similar experimental study that demonstrated the enhancement of water absorption rate by the substitution of cement in concrete with natural zeolite [32].

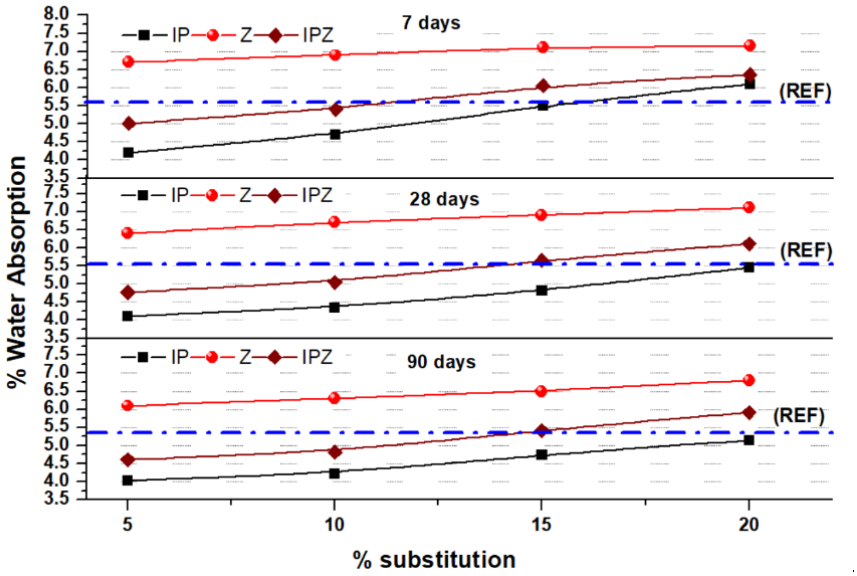

Figure 11. Percentage water absorption vs admixture concentration

3.6. Acid Attack and Sulphate Attack Test

The compressive strength test findings done at 28, 90, and 120 days following exposure to sulphate attack are illustrated in Figure 12. The concrete specimens containing IP exhibited a more significant decrease in strength. When compared to normal concrete, IP 20 concrete saw a 16.67% greater percentage rise in the loss of compressive strength at 120 days. This finding indicates that the concrete mixture including zeolite as a substitute for cement exhibited greater resistance to sulphate attack compared to the other two combinations. In the context of the IPZ concrete series, it was seen that the compressive strength exhibited a notable decline. Nevertheless, it was found that this reduction was comparatively smaller when compared to the loss observed in concrete containing IP. A significant increase of 8.3% in compressive strength decrease was seen in IPZ 20 when compared to standard concrete.

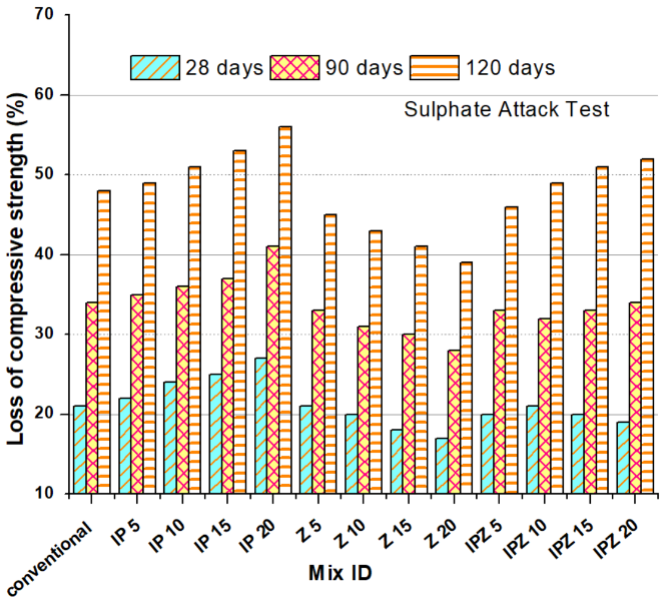

Figure 12. Loss of compressive strength of concrete mixes due to sulphate attack

In the acid attack test, a graph pattern similar to that of the sulphate attack test results was observed, as shown in Figure 13. This could be a result of the acidic environment reacting with $Ca(OH)_2$ to influence the formation of CSH gel [33]. The corrosive effects of acid environments result in a more significant reduction in strength when compared to the impact of sulphate attack conditions. The reaction between cement pastes and sulphuric acid results in the formation of calcium sulphate, which is a highly soluble salt. The degradation of concrete structure is attributed to the specific action of calcium chloride on the cement paste. Concrete with an alumina silicate link has a reduction in strength when subjected to acid or sulphate attack. Hence, it has been seen via several studies that the utilization of river sand in

concrete results in enhanced resistance against acid or sulphate environments [6]. Figure 14 depicts the mass loss resulting from sulphate attack and acid attack over a period of 120 days. Hence, it is possible that IPZ concrete may not be appropriate for areas that are prone to acid and sulphate degradation, which is also reflected in previous studies [34].

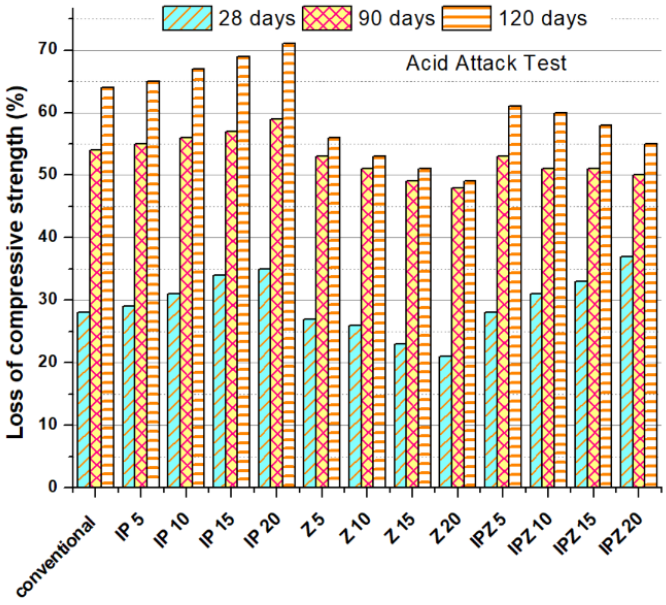

Figure 13. Loss of compressive strength of concrete mixes due to acid attack

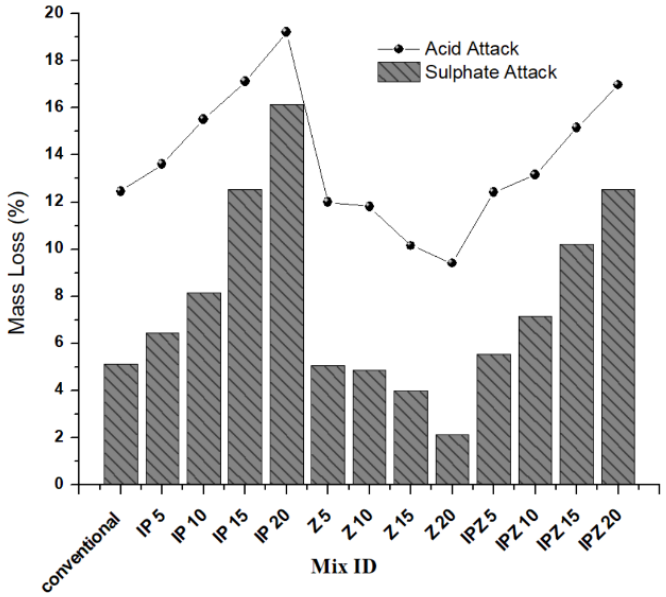

Figure 14. Mass loss of concrete mixes due to acid attack and sulphate attack

3.7. Rapid Chloride Ion Penetration Test

Figure 15 displays the test outcomes pertaining to the rapid chloride ion penetration values of both control concrete and concrete specimens containing admixtures. As the concentration of the admixture increases, there is a corresponding decrease in charge penetrability. The observation was made that the inclusion of IPZ admixtures in concrete resulted in a greater resistance to charge penetration when compared to the other combinations. The charges employed exhibited temperatures ranging from 1000 °C to 2000 °C for IPZ 20 and IPZ 15. According to the ASTM C1202 (2012) standard, it was categorized as exhibiting a low level of chloride penetration. The enhanced fineness of the material exhibits improved resistance against the infiltration of chloride ions under external forces. Therefore, the substitution of cement with zeolite and sand with IP is expected to have a positive and significant impact on the infiltration of chloride ions in concrete. Similar to this, the coulomb charge in the concrete specimen decreased as the number of curing days increased. For the 90-day curing period, all charges passed for the control concrete, IP concrete, zeolite concrete, and IPZ concrete mix were lower than for the control concrete. Previous studies demonstrated that the use of IP in recycled aggregate concrete reduces the pore volume and creates isolated micro voids which arrest the tortuosity of the concrete [35].

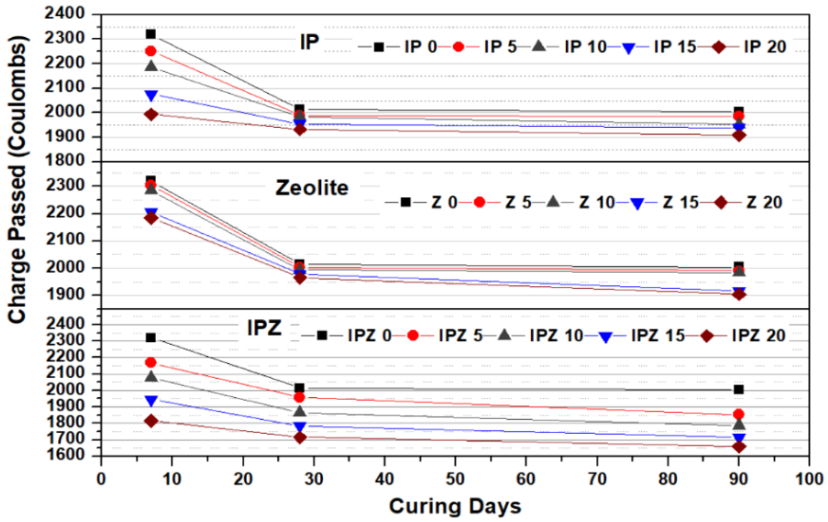

Figure 15. Charge passed vs. curing days of various concrete mix

3.8. Modulus of Elasticity

Figure 16 illustrates the modulus of elasticity after a cure period of 28 days. The modulus of elasticity of concrete changed with admixtures and exhibited a higher value compared to the control concrete. The modulus of elasticity shows a respective increase of 4.78%, 6.68%, and 15.48% for IP20, Z20, and IPZ 20 in comparison to the control concrete. The experimental results clearly indicate that the incorporation of IP and zeolite in concrete resulted in the highest modulus of elasticity. This phenomenon may be attributed to the enhanced intermolecular forces between the aggregates and the constituent material inside the mixture, leading to an augmentation in compressive strength, ultrasonic pulse velocity (UPV) values, split tension, and flexural strength. The findings from the modulus of elasticity test exhibited a strong resemblance to the observed pattern in the results of the compressive strength test. This finding illustrates a substantial correlation between compressive strength and modulus of elasticity. Previous studies have also demonstrated a quantitative relationship between compressive stress and modulus of elasticity, with IP serving as a variable parameter [34].

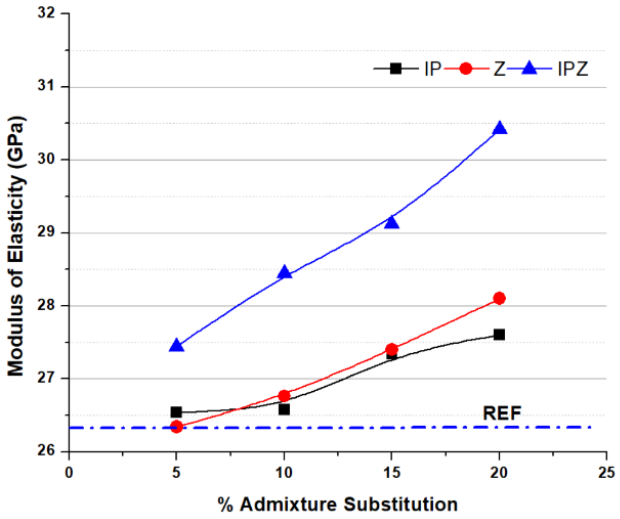

Figure 16. Modulus of elasticity vs. admixture concentration

3.9. Drying Shrinkage

Figure 17 depicts the drying and shrinkage characteristics of all concrete mixes. The study revealed that concrete with a higher percentage of additives exhibited less drying shrinkage. The drying shrinkage of IP20, Z20, and IPZ20 exhibited reductions of 57.9%, 49.7%, and 60.3%, respectively, in comparison to the control concrete. The drying shrinkage of concrete is reduced as the concentration of additives increases. This observation illustrates that the incorporation of IP into the concrete served as a filler, given that the particle size was lower compared to that of sand, leading to an enhanced pore arrangement. The test results show a high degree of similarity when compared to the findings of Zhang et al. [36]. Similarly, the elevated porosity of IP and zeolite facilitates the absorption of a greater quantity of water during the mixing phase, hence providing an additional water supply during the subsequent drying

process. Zeolite is a naturally occurring mineral characterized by its substantial surface area and unique framework, which facilitate its capacity to adsorb and hold water molecules. Zeolite, when used as an addition in concrete, serves as a water reservoir, mitigating the shrinkage resulting from the dehydration that occurs during the curing phase. Zeolite has the ability to hold water, which can aid in the maintenance of a more uniform moisture level in concrete, thereby mitigating the occurrence of drying shrinkage. Furthermore, the capacity of zeolite to facilitate ion exchange might augment the hydration mechanism and boost the overall robustness and endurance of concrete. Singh et al. (2013) conducted a study in which they found that small particles derived from coal bottom ash had a notable water-holding ability. This characteristic has been seen to effectively restrict the occurrence of curing shrinkage in concrete, hence enhancing its performance [37]. The process of filling the holes and voids in concrete with tiny particles effectively impedes the development of harmful micro cracks [38].

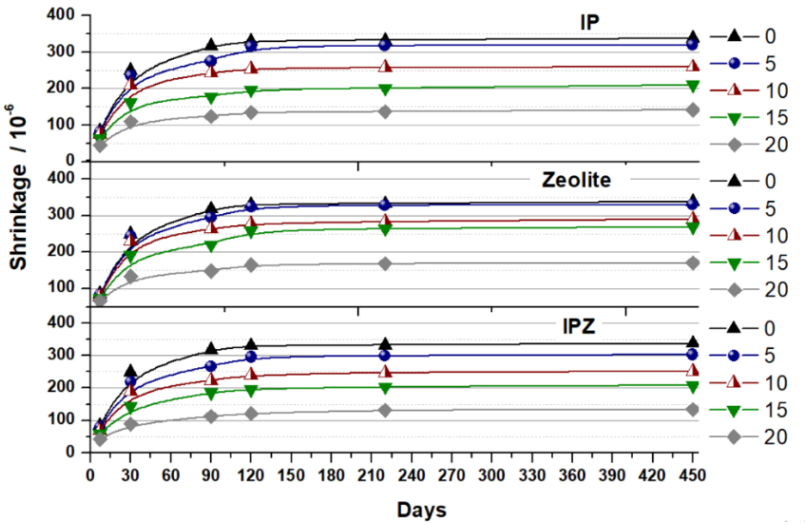

Figure 17. Duration vs. shrinkage of various concrete mix

3.10. Thermal Conductivity

The thermal conductivity values of each concrete mixture are illustrated in Figure 18. A reduction in thermal conductivity was seen with an increase in admixture content. The heat conductivity rating of IP20 concrete was found to be the lowest. The thermal conductivity of IP20 and IPZ20 concrete exhibits a reduction of 8.27% compared to that of normal concrete. In comparison to normal concrete, the inclusion of zeolite in concrete reduces heat conductivity, albeit only by 3.57 percent. The thermal conductivity of concrete is influenced by its density, which in turn affects the amount of heat transfer. The intricate structure and higher solid content resulted from the reduction of voids in the concrete, which leads to increased thermal resistance [39]. The specific heat capacity of iron ore powder is 570 J/kgK [24]. Which is lower than the specific heat capacity of concrete; consequently, the thermal conductivity decreases as the admixture concentration increases. According to comparable test results reported by Eva et al., the addition of natural zeolite to cement enhances the thermal resistance of concrete. The limited specific heat capacity of zeolite decreases the thermal conductivity of concrete [40]. Therefore, the incorporation of IPZ into concrete permits its use in applications requiring thermal resistance.

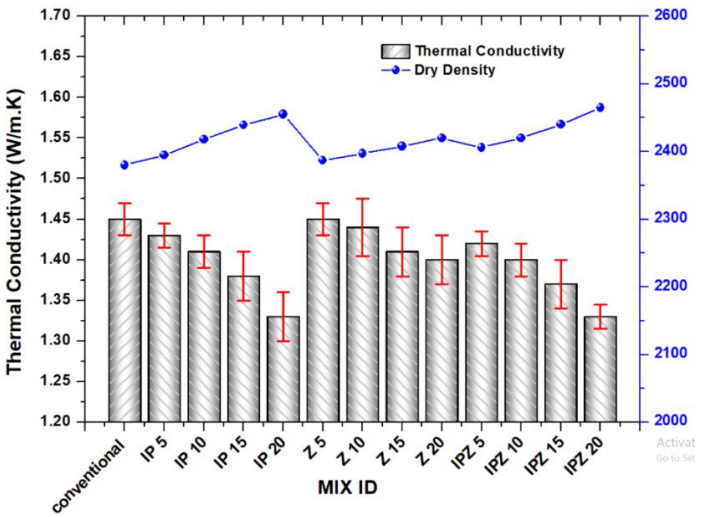

Figure 18. Thermal conductivity of all the concrete mix

4. Cost Analysis

A comparative cost study was undertaken to ascertain the economic benefits associated with the utilization of IP and Z in concrete. Table 4 presents a comparison between the production costs of 1 m^3 of conventional concrete and 1 m^3 of admixture-modified concrete with a 20% inclusion of IPZ. The comparative analysis of production costs between conventional concrete and IPZ concrete provides clear evidence that it is feasible to lower building expenses, reduce cement consumption, and minimize the use of river sand in concrete production. This, in turn, contributes to the mitigation of river sand mining activities. From an environmental standpoint, the challenges related to the disposal of iron ore waste may be addressed by employing IP as a cost-effective alternative to sand as a filler and zeolite as a substitute for cement in concrete.

Table 4. Quantity estimates and corresponding cost for producing 1m3 of conventional concrete and IPZ20 concrete

Mix	Materials used	Price/unit (INR)	Quantity required (m3)	Cost (Rs.)
Conventional concrete	Cement	469/50 kg bag	420	3940
	Sand	85/cubic feet	624	332.6
	Coarse aggregate	1100/Ton	1218	1339.8
	Water	30/kl	168	5.04
	Conplast SP 430	45/kg	4.2	189
Total Cost				**5806.44**
IPZ 20	Cement	469/50 kg bag	336	3151.68
	Sand	85/cubic feet	498	265.44
	Coarse aggregate	1100/Ton	1218	1339.8
	Water	30/kl	168	5.04
	Conplast SP 430	45/kg	42	189
	IP	0	126	0
	Zeolite	0	84	0
Total Cost				**4950.96**

The computation did not incorporate the expenses associated with the transportation and calcination of iron ore particles and zeolites. The inclusion of a contingency fee of up to Rs. 20/kg is contingent upon the distance of the site location. It is imperative to acknowledge that the efficacy of zeolite in mitigating shrinkage is subject to variation, contingent upon elements like the precise type and dose of zeolite employed, the concrete's mix design, and prevailing climatic conditions. Hence, it is advisable to do targeted experiments and seek guidance from specialists or pertinent studies in order to ascertain the most effective application of zeolite in concrete for mitigating shrinkage in a given context.

5. Conclusions

The study focused on examining the strength and durability attributes of M20-grade concrete that incorporated iron ore tailing powder (IP) and zeolite (Z) as partial replacements for sand and cement, respectively. The investigation assessed various aspects of the concrete, including its workability in the fresh state, mechanical characteristics such as compressive strength, flexural strength, split tensile strength, ultrasonic pulse velocity, and durability characteristics such as permeability, water absorption test, rapid chloride ion penetration, and drying shrinkage. The experiments undertaken yielded the following conclusions:

- The high water-holding capacity of IP and zeolite increased the water demand in the concrete mix. Consequently, the workability of the concrete was diminished. However, the slump values for all admixture-modified concrete fall within the medium slump range. In terms of workability, it is advised that the IP and Z admixtures dosage not exceed 20%.
- IPZ20-containing concrete showed the highest compressive, flexural, and split tensile strengths. Higher UPV readings are due to higher density and particle packing. Strength increases suggest both admixtures are pozzolanic.
- Similarly, the modulus of elasticity of IPZ20 was 15.48% greater than that of conventional concrete. This demonstrates that IPZ concrete has a high stress-bearing capacity with minimal deformation. In addition, the drying shrinkage of IPZ20 concrete was significantly less than that of the standard control mix and demonstrated exceptional resistance to sulphate and acid attacks. The decrease in water absorption and chloride ion penetration indicates that IPZ20 concrete has fewer voids than control concrete.

- The cost analysis also demonstrated that it is possible to produce cost-effective concrete with minimal environmental impact while maintaining economic viability. In future research, the contribution of IP and zeolite to the modification of the microstructure of the concrete can be investigated in depth.

Thus, it is possible to conclude that IPZ20 concrete containing 10% zeolite as a cement replacement and 10% iron ore tailing powder as a sand replacement is a viable alternative to pozzolanic materials. In addition, using iron ore tailing powder in concrete will be an eco-friendly method to dispose of waste iron ore tailing powder and preserve the environment.

6. Declarations

6.1. Author Contributions

Conceptualization, K.K.P. and M.A.; methodology, K.K.P.; validation, K.K.P. and M.A.; formal analysis, M.A.; investigation, K.K.P.; resources, K.K.P.; data curation, M.A.; writing—original draft preparation, K.K.P.; writing—review and editing, M.A.; visualization, K.K.P.; supervision, M.A.; project administration, M.A. All authors have read and agreed to the published version of the manuscript.

6.2. Data Availability Statement

Data sharing is not applicable to this article.

6.3. Funding

The authors received no financial support for the research, authorship, and/or publication of this article.

6.4. Acknowledgements

The corresponding author would like to acknowledge the management of Francis Xavier Engineering College for providing proper support for the research work and all the teaching and non-teaching fraternities who helped throughout the execution of the work. Also, would like to express my gratitude to my family members for their continuous encouragement and motivation to achieve in my research career.

6.5. Conflicts of Interest

The authors declare no conflict of interest.

7. References

[1] Yang, G., Deng, Y., & Wang, J. (2014). Non-hydrothermal synthesis and characterization of MCM-41 mesoporous materials from iron ore tailing. Ceramics International, 40(5), 7401–7406. doi:10.1016/j.ceramint.2013.12.086.

[2] U.S Geologicial Survey. (2020). Iron ore 2020. US Geological Survey, Mineral Commodity Summaries, U.S Geologicial Survey, Reston, United States.

[3] Das, S. K., Kumar, S., & Ramachandrarao, P. (2000). Exploitation of iron ore tailing for the development of ceramic tiles. Waste Management, 20(8), 725–729. doi:10.1016/S0956-053X(00)00034-9.

[4] Liu, Y., Du, F., Yuan, L., Zeng, H., & Kong, S. (2010). Production of lightweight ceramisite from iron ore tailings and its performance investigation in a biological aerated filter (BAF) reactor. Journal of Hazardous Materials, 178(1–3), 999–1006. doi:10.1016/j.jhazmat.2010.02.038.

[5] Du, Z., Ge, L., Ng, A. H. M., Zhu, Q., Horgan, F. G., & Zhang, Q. (2020). Risk assessment for tailings dams in Brumadinho of Brazil using InSAR time series approach. Science of the Total Environment, 717, 137125. doi:10.1016/j.scitotenv.2020.137125.

[6] Shettima, A. U., Hussin, M. W., Ahmad, Y., & Mirza, J. (2016). Evaluation of iron ore tailings as replacement for fine aggregate in concrete. Construction and Building Materials, 120, 72–79. doi:10.1016/j.conbuildmat.2016.05.095.

[7] Prakash, S., Das, B., Mohapatra, B. K., & Venugopal, R. (2000). Recovery of iron values from iron ore slimes by selective magnetic coating. Separation Science and Technology, 35(16), 2651–2662. doi:10.1081/SS-100102361.

[8] Peiravi, M., Dehghani, F., Ackah, L., Baharlouei, A., Godbold, J., Liu, J., Mohanty, M., & Ghosh, T. (2021). A Review of Rare-Earth Elements Extraction with Emphasis on Non-conventional Sources: Coal and Coal Byproducts, Iron Ore Tailings, Apatite, and Phosphate Byproducts. Mining, Metallurgy and Exploration, 38(1), 1–26. doi:10.1007/s42461-020-00307-5.

[9] Yang, C., Cui, C., Qin, J., & Cui, X. (2014). Characteristics of the fired bricks with low-silicon iron tailings. Construction and Building Materials, 70, 36–42. doi:10.1016/j.conbuildmat.2014.07.075.

[10] Mendes, B. C., Pedroti, L. G., Fontes, M. P. F., Ribeiro, J. C. L., Vieira, C. M. F., Pacheco, A. A., & Azevedo, A. R. G. d. (2019). Technical and environmental assessment of the incorporation of iron ore tailings in construction clay bricks. Construction and Building Materials, 227, 116669. doi:10.1016/j.conbuildmat.2019.08.050.

[11] Wu, D., Sun, W., Liu, S., & Qu, C. (2021). Effect of microwave heating on thermo-mechanical behavior of cemented tailings backfill. Construction and Building Materials, 266. doi:10.1016/j.conbuildmat.2020.121180.

[12] Gu, X., Zhang, W., Zhang, X., Li, X., & Qiu, J. (2022). Hydration characteristics investigation of iron tailings blended ultra-high performance concrete: The effects of mechanical activation and iron tailings content. Journal of Building Engineering, 45, 103459. doi:10.1016/j.jobe.2021.103459.

[13] Han, P. (2013). Experimental Study on High Silicon Iron Ore Tailings Effect on Concrete Workability and Compressive Strength. Northeastern University, Boston, United States.

[14] Zhang, N., Tang, B., & Liu, X. (2021). Cementitious activity of iron ore tailing and its utilization in cementitious materials, bricks and concrete. Construction and Building Materials, 288, 123022. doi:10.1016/j.conbuildmat.2021.123022.

[15] Seraj, S., Ferron, R. D., & Juenger, M. C. G. (2016). Calcining natural zeolites to improve their effect on cementitious mixture workability. Cement and Concrete Research, 85, 102–110. doi:10.1016/j.cemconres.2016.04.002.

[16] Uzal, B., Turanli, L., Yücel, H., Göncüoğlu, M. C., & Çulfaz, A. (2010). Pozzolanic activity of clinoptilolite: A comparative study with silica fume, fly ash and a non-zeolitic natural pozzolan. Cement and Concrete Research, 40(3), 398–404. doi:10.1016/j.cemconres.2009.10.016.

[17] Caputo, D., Liguori, B., & Colella, C. (2008). Some advances in understanding the pozzolanic activity of zeolites: The effect of zeolite structure. Cement and Concrete Composites, 30(5), 455–462. doi:10.1016/j.cemconcomp.2007.08.004.

[18] Chan, S. Y. N., & Ji, X. (1999). Comparative study of the initial surface absorption and chloride diffusion of high-performance zeolite, silica fume and PFA concretes. Cement and Concrete Composites, 21(4), 293–300. doi:10.1016/S0958-9465(99)00010-4.

[19] Ahmadi, B., & Shekarchi, M. (2010). Use of natural zeolite as a supplementary cementitious material. Cement and Concrete Composites, 32(2), 134–141. doi:10.1016/j.cemconcomp.2009.10.006.

[20] Karakurt, C., & Topçu, I. B. (2011). Effect of blended cements produced with natural zeolite and industrial by-products on alkali-silica reaction and sulfate resistance of concrete. Construction and Building Materials, 25(4), 1789–1795. doi:10.1016/j.conbuildmat.2010.11.087.

[21] Fernandez, R., Martirena, F., & Scrivener, K. L. (2011). The origin of the pozzolanic activity of calcined clay minerals: A comparison between kaolinite, illite and montmorillonite. Cement and Concrete Research, 41(1), 113–122. doi:10.1016/j.cemconres.2010.09.013.

[22] Vigil De La Villa, R., Fernández, R., Rodríguez, O., García, R., Villar-Cociña, E., & Frías, M. (2013). Evolution of the pozzolanic activity of a thermally treated zeolite. Journal of Materials Science, 48(8), 3213–3224. doi:10.1007/s10853-012-7101-z.

[23] Elkady, H., Serag, M. I., & Elfeky, M. S. (2013). Effect of nano silica de-agglomeration, and methods of adding super-plasticizer on the compressive strength, and workability of nano silica concrete. Civil and Environmental Research, 3(2), 21-34.

[24] Masdeu, F., Carmona, C., Horrach, G., & Muñoz, J. (2021). Effect of Iron (III) Oxide Powder on Thermal Conductivity and Diffusivity of Lime Mortar. Materials, 14(4), 998. doi:10.3390/ma14040998.

[25] Yellishetty, M., Karpe, V., Reddy, E. H., Subhash, K. N., & Ranjith, P. G. (2008). Reuse of iron ore mineral wastes in civil engineering constructions: A case study. Resources, Conservation and Recycling, 52(11), 1283–1289. doi:10.1016/j.resconrec.2008.07.007.

[26] Hou, Y. (2014). Comparison of effect of iron tailing sand and natural sand on concrete properties. Key Engineering Materials, 599, 11–14. doi:10.4028/www.scientific.net/KEM.599.11.

[27] Goyal, S., Singh, K., Hussain, A., & Singh, P. R. (2015). Study on partial replacement of sand with iron ore tailing on compressive strength of concrete. International Journal of Research in Engineering & Advanced Technology, 3(2), 243–248.

[28] Vaičiukynienė, D., Skripkiūnas, G., Sasnauskas, V., & Daukšys, M. (2012). Cement compositions with modified hydrosodalite. Chemija, 23(3), 147–154.

[29] Zhao, J., Wang, Q., Xu, G., Shi, Y., & Su, Y. (2023). Influence of macro-synthetic fiber on the mechanical properties of iron ore tailing concrete. Construction and Building Materials, 367, 130293. doi:10.1016/j.conbuildmat.2023.130293.

[30] Zhang, Y., Li, Z., Gu, X., Nehdi, M. L., Marani, A., & Zhang, L. (2023). Utilization of iron ore tailings with high volume in green concrete. Journal of Building Engineering, 72, 106585. doi:10.1016/j.jobe.2023.106585.

[31] Correia, J. R., De Brito, J., & Pereira, A. S. (2006). Effects on concrete durability of using recycled ceramic aggregates. Materials and Structures/Materiaux et Constructions, 39(2), 169–177. doi:10.1617/s11527-005-9014-7.

[32] Valipour, M., Pargar, F., Shekarchi, M., & Khani, S. (2013). Comparing a natural pozzolan, zeolite, to metakaolin and silica fume in terms of their effect on the durability characteristics of concrete: A laboratory study. Construction and Building Materials, 41, 879–888. doi:10.1016/j.conbuildmat.2012.11.054.

[33] Bakharev, T., Sanjayan, J. G., & Cheng, Y. B. (2003). Resistance of alkali-activated slag concrete to acid attack. Cement and Concrete Research, 33(10), 1607–1611. doi:10.1016/S0008-8846(03)00125-X.

[34] Liu, K., Wang, S., Quan, X., Jing, W., Xu, J., Zhao, N., & Liu, B. (2022). Effect of iron ore tailings industrial by-product as eco-friendly aggregate on mechanical properties, pore structure, and sulfate attack and dry-wet cycle's resistance of concrete. Case Studies in Construction Materials, 17. doi:10.1016/j.cscm.2022.e01472.

[35] Xu, F., Wang, S., Li, T., Liu, B., Zhao, N., & Liu, K. (2021). The mechanical properties and resistance against the coupled deterioration of sulfate attack and freeze-thaw cycles of tailing recycled aggregate concrete. Construction and Building Materials, 269, 121273. doi:10.1016/j.conbuildmat.2020.121273.

[36] Zhang, G. D., Zhang, X. Z., Zhou, Z. H., & Cheng, X. (2014). Preparation and properties of concrete containing iron tailings/manufactured sand as fine aggregate. Advanced Materials Research, 838–841, 152–155. doi:10.4028/www.scientific.net/AMR.838-841.152.

[37] Singh, M., & Siddique, R. (2013). Effect of coal bottom ash as partial replacement of sand on properties of concrete. Resources, Conservation and Recycling, 72, 20–32. doi:10.1016/j.resconrec.2012.12.006.

[38] Krishna Kumar, P., & Chinnaraju, K. (2022). Utilization potentials of a nano bio-carbonate filler to mitigate alkali-aggregate reactivity of glass powder–foamed concrete. Canadian Journal of Civil Engineering, 49(10), 1569–1581. doi:10.1139/cjce-2022-0122.

[39] Palaniappan, K. K., Komarasamy, C., & Murugan, S. (2022). Utilization of Cuttlebone as Filler in Hydrophobic Foam Mortar: A Technical and Economical Feasibility Study. Journal of Materials in Civil Engineering, 34(8), 4022191. doi:10.1061/(asce)mt.1943-5533.0004335.

[40] Vejmelková, E., Koňáková, D., Kulovaná, T., Keppert, M., Žumár, J., Rovnaníková, P., Keršner, Z., Sedlmajer, M., & Černý, R. (2015). Engineering properties of concrete containing natural zeolite as supplementary cementitious material: Strength, toughness, durability, and hygrothermal performance. Cement and Concrete Composites, 55, 259–267. doi:10.1016/j.cemconcomp.2014.09.013.